Effect of power feature covariance shift on BCI spatial-filtering techniques: A comparative study

Aleksandar Miladinović[1], Miloš Ajčević[1], Joanna Jarmolowska[2], Uros Marusic[3,4], Marco Colussi[2], Giulia Silveri[1], Piero Paolo Battaglini[2], Agostino Accardo[1]

[1]*Department of Engineering and Architecture, University of Trieste, Via Alfonso Valerio 10, 34127, Trieste, Italy*

[2]*Department of Life Sciences, B.R.A.I.N. Center for Neuroscience, University of Trieste, Via Alexander Fleming 22, 34127 Trieste, Italy*

[3]*Science and Research Centre Koper, Institute for Kinesiology Research, Garibaldijeva 1, 6000, Koper, Slovenia*

[4]*Department of Health Sciences, Alma Mater Europaea - ECM, Slovenska ulica 17, 2000, Maribor, Slovenia*

Corresponding author: Aleksandar Miladinović
Department of Engineering and Architecture, University of Trieste
Via A. Valerio 10, Trieste – 34127, Italy
Email: aleksandar.miladinovic@phd.units.it
Phone: +39 040.558.7130

Manuscript version: **Accepted Manuscript**
© 2020. This manuscript version is made available under the CC-BY-NC-ND 4.0 license
http://creativecommons.org/licenses/by-nc-nd/4.0/

The final authenticated version is available online at: https://doi.org/10.1016/j.cmpb.2020.105808

Abstract: (350 words)

Background and Objective

The input data distributions of EEG-based BCI systems can change during intra-session transitions, due to nonstationarity caused by features covariate shifts, thus compromising BCI performance.
We aimed to identify the most robust spatial filtering approach, among most used methods, testing them on calibration dataset, and test dataset recorded 30 min afterwards. In addition, we also investigated if their performance improved after application of Stationary Subspace Analysis (SSA).

Methods

We have recorded, in 17 healthy subjects, the calibration set at the beginning of the upper limb motor imagery BCI experiment and testing set separately 30 min afterwards. Both the calibration and test data were pre-processed and the BCI models were produced by using several selected spatial filtering approaches on the calibration set. Those models were subsequently evaluated on a test set. The differences between the accuracy estimated by cross-validated on the calibration dataset and accuracy on the test dataset were investigated. The same procedure was performed with, and without SSA pre-processing step.

Results

A significant reduction in accuracy on the test dataset was observed for CSP, SPoC and SpecRCSP. For SLap, SpecCSP only a slight decreasing trend was observed, while FBCSP and FBCSPT largely maintained moderately high median accuracy >70%. In the case of application of SSA pre-processing the differences between accuracy observed on calibration and test dataset were reduced. In addition, accuracy values both on calibration and test set were slightly higher in case of SSA pre-processing and also in this case FBCSP and FBCSPT presented slightly better performance compared to other methods.

Conclusion

The intrinsic signal nonstationarity characteristics, caused by covariance shifts of power features reduced the accuracy of BCI model suggesting that this evaluation framework should be considered for testing simulating real life performance. FBCSP and FBSCPT approaches showed to be more robust to feature covariance shift. SSA can improve the models performance and reduce accuracy decline from calibration to test set.

Keywords

BCI, EEG, spatial filtering, covariance shift, motor-imagery

Highlights

- *This study investigates the performance of several spatial-filtering approaches on calibration and test set acquired 30 min after the calibration, mimicking the real BCI scenarios.*
- *EEG extracted feature covariance shifts lead to the BCI model accuracy deterioration, even after 30 minutes of a break.*
- *FBCSP and FBSCPT showed to be more robust to feature covariance shift largely maintaining the original performance characterized by moderately high accuracy (>70%).*
- *Stationary Subspace Analysis pre-processing improved the models performance and also reduced the gap between calibration and test set observed BCI model accuracies.*

1. Introduction

The use of noninvasive EEG brain-computer interfaces (BCI) application has increased in the last few years. Today due to advanced techniques of signal processing and hardware accessibility we are able to create more reliable systems that open space for the development of innovative clinical and non-clinical BCI procedures [1–4].

Various studies [5–7] reported induced changes on sensorimotor rhythms and positive effects of different BCI treatment approaches on different pathologies, such as Parkinson's disease [8,9], Stroke [10] Autism-spectrum disorder [11,12], ADHD [13], etc. However, it is natural that the effectiveness of BCI treatment is also related to the technical realization of the system and its capability of detecting EEG sensorimotor rhythms (SMR) generated during Motor-Imagery (MI) used as a feedback signal.

The correct interpretation of the neural information extracted from electroencephalogram (EEG) is a cornerstone of the sensorimotor BCI. Therefore, is of great importance enhancing sensitivity to particular brain sources, improving source localization and suppressing artifacts [14]. The proper channel selection realized by applying spatial filtering plays a pivotal role in making a system more sensitive to SMR, and less sensitive to other non-related brain activities and noises. Spatial filters and their application in BCI were largely studied [15–20]. Data-independent spatial filters like Surface Laplacian with fixed weights [15,21,22] were largely used due to its simplicity, but it was found sensitive to anatomical differences and cross-subject variability [23,24]. Data-driven filters spatial such as CSP and its variants were designed to overcome the aforementioned limits. On the other side, it is also reported [18] that CSP is sensitive towards noisy training data [25], nonstationarities [26] and small datasets [27,28]. Most BCI studies related to spatial filtering techniques were based only on the evaluation performed on calibration (training) and test set derived from the same EEG recording. In real-life BCI applications, the online session is performed about 20 minutes after the initial calibration session and therefore disregard a time-varying feature's distribution, such as intrinsic signal nonstationarity characteristic for EEG, caused by power feature covariance shifts [29,30], that compromise BCI performance.

Therefore, the aim of our study was to identify the most robust spatial filtering approach, among most used methods, in the real BCI procedure testing them on data deriving from two different recording sessions in order to test how nonstationarity affects their performance. In addition, we also investigated if their performance improved after application of stationary subspace analysis.

2. Materials and Methods

2.1 Study population

Twenty healthy subjects have participated in the study (age range 19–26 years, mean±1SD = 22 ± 1.9). All subjects were right-handed, BCI naïve and with no history of neurological disorders, and in particular without impaired motor functions.

The study was conducted within the MEMORI-net Interreg V-A ITS-SLO project. All recruited subjects gave their signed informed consent to participate in the study. The study protocol was approved by the Regional Ethical Committee CEUR (Comitato Etico Unico Regionale, FVG, Italy) with approval number 118/2018. The research was conducted according to the principles of the Declaration of Helsinki.

2.2 Study design and BCI protocol

To emphasize the real-life Motor-Imagery BCI (MI-BCI) scenarios we have recorded training and testing set separately. The training set had been collected at the beginning of the experiment, whereas the test set subsequently has been acquired 30min afterwards, as in Figure 1A. During the break, the participants were resting in a chair.

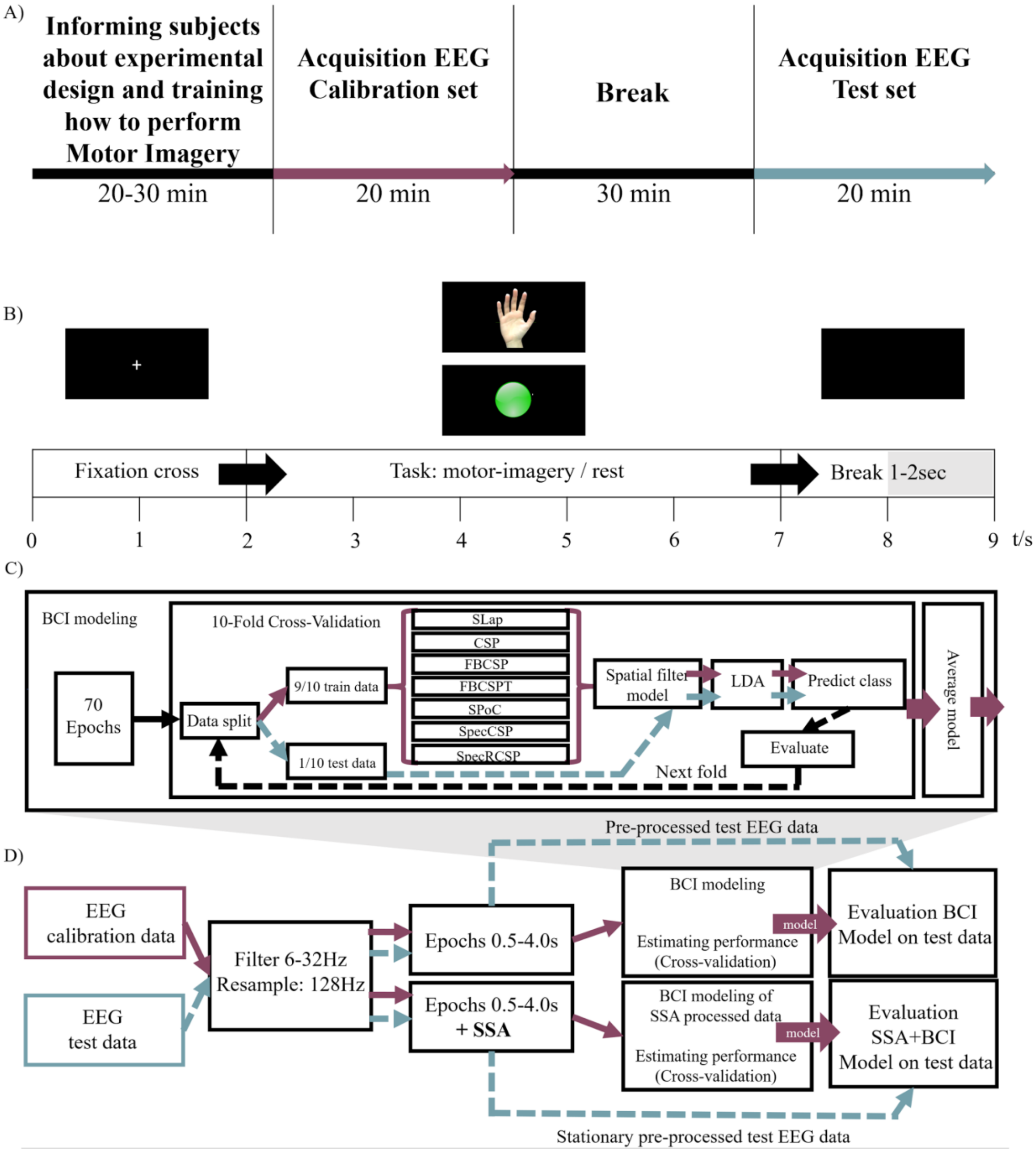

Figure 1. A) Graphical representation of the experimental design; B) Time-sequence of stimuli presentation; C) BCI modelling block diagram; D) Block-diagram of applied BCI processing steps. Dark pink color and shadow green represent the processing pipeline of calibration data and test data, respectively. Both the calibration and test data were pre-processed and the produced models on the calibration set were additionally evaluated on a test set. The same procedure was performed with and without stationary subset analysis (SSA) pre-processing step.

For both calibration and test dataset, subjects had to perform 70 tasks (35 repetitions of right-hand MI task and 35 reparations of "rest" task, randomly), as in Figure 1B. The stimulus consisted of the fixation cross on the screen to draw participant attention for two seconds, followed by the instruction to imagine the right hand (MI) or stay in "rest" and it was presented for 5 seconds (Figure 1B). The inter-trial period was from 1 to 2 seconds. The adopted single right-hand vs "rest" design was chosen considering the applications of BCI techniques in neurorehabilitation to target a specific motor area during a specific rehabilitation task, as reported previously [3,31,32]. Both conditions (MI and "rest") had the same size of 5 seconds, as shown in Figure 1 B. For the MI task the still image of the right hand was presented, while for the "rest" condition the green circle was displayed.

The experiment was performed, and data was acquired by locally designed software "NeuroTS" available at https://github.com/miladinovic/NeuroTS. The NeuroTS allows both stimulus presentation for calibration and feedback for online sessions. In this study we used only stimuli presentation feature, both during calibration and test sessions.

The acquisition of 12 channel EEG was performed using SAM 32FO amplifier (Micromed S.p.A., Italy) and Ag/AgCl electrodes (FC3, FC4, C4, C3, CP3, CP4, C2, C4, C6, C5, O1, O2). The signals were recorded with 256 Hz sample frequency and subsequently pre-processed with the 6-32Hz 4th order Butterworth bandpass filter and resampled to 128Hz. The signal was epoched from 0.5 to 4.5 seconds relative to the presentation of the cue on the screen.

The aforementioned evaluation procedure was performed firstly without SSA pre-processing, as a standard procedure, and secondly with SSA pre-processing.

The pre-processing step included initial resampling, filtering and epoching before the BCI modelling (Figure 1C and 1D). The procedure was performed firstly without Stationary Subspace Analysis (SSA) pre-processing, as a standard procedure, and secondly with SSA pre-processing (Figure 1D). Subsequent BCI modelling (Figure 1C) performed both with and without SSA, encompassed spatial filtering, feature extraction and classification, and has been performed on the EEG sensor space. The BCI modelling has been performed on the selected approaches and their performances have been estimated using cross-validation. Finally, for the real model performances have been evaluated on the separate EEG test set.

2.3 Stationary Subspace Analysis

The additional pre-processing of factorization of the multivariate EEG data into its stationary and non-stationary components has been performed with the analytical Stationary Subspace Analysis algorithm presented in [33,34]. In particular, we assume that the system with D sources consists of d stationary source signals $s^{\mathbb{s}}(t) = [s_1(t), s_2(t), \dots, s_d(t)]^\top$(named $\mathbb{s}$-sources) and D - d nonstationary source signals $s^{\mathbb{m}}(t) = [s_{d+1}(t), s_{d+2}(t), \dots, s_D(t)]^\top$(also named $\mathbb{m}$-sources). The observed signals $x(t)$ can expressed as a linear superposition of the sources that are non necessary independent, and A is an invertible matrix

$$x(t) = As(t) = [A^{\mathbb{s}} \quad A^{\mathbb{m}}][s^{\mathbb{s}}(t)\ s^{\mathbb{m}}(t)]^T, \quad (1)$$

The spaces spanned by $A^{\mathbb{s}}$ and $A^{\mathbb{m}}$are called $\mathbb{s}$- and $\mathbb{m}$-space, respectively. The goal is to find a linear transformation $\hat{A}^{-1}$that separates the $\mathbb{s}$-sources from the $\mathbb{m}$-sources, factorizing $x(t)$ according to Eq. (1). Therefore, we write the estimated demixing matrix as $\hat{A}^{-1}$=$\hat{B}$W where $W = Cov(x)^{-\frac{1}{2}}$is a whitening matrix and $\hat{B}$ is an orthogonal matrix.

An optimization procedure [33,34] was used to determine the rotation part of $\hat{B}$ during which the first d components of estimated sources $\hat{s}(x) = \hat{B}Wx(t)$, are as stationary as possible.

Therefore, we divided the data into N consecutive epochs $X_1, \dots, X_N \subset \Re^D$and selected estimated sources as stationary if their joint distribution didn't change over all epochs. The detailed explanation of the algorithm can be found in [34].

In our work, the SSA pre-processing has been performed as an additional step before applying spatial filtering, as proposed in [35]. Before applying the SSA, EEG was epoched to MI and "rest" tasks, to ensure that differences between "rest" and MI are not counted as non-stationarity. Finally, the algorithm outputs the set of ranked twelve sources according to their stationarity, and 70% of them have been selected for further BCI modelling, whereas 30% marked as non-stationary were discarded. The 70-30% cut-off, which was fixed for all participants and methods, was considered as a best trade-off between a discriminatory power of the model and the maintenance of the performance (accuracy) over time.

2.4 BCI approaches

In this study the following approaches were included: Surface Laplacian (SLap), Common Spatial Pattern (CSP), Filter Bank Common Spatial Pattern (FBCSP), Filter Bank Common Spatial Pattern Time (FBCSPT), Source Power Co-modulation (SPoC), Spectrally Weighted Common Spatial Patterns (SpecCSP), Spectrally Weighted Regularized Common Spatial Patterns (SpecRCSP). All aforelisted approaches fulfilled the following inclusion criteria: 1) noise robustness, 2) reported resilience to a non-stationarity between calibration data and online data 3) processing delay (the maximal real-time cannot exceed 300ms), 4) required a number of channels (up to 16), 4) required parametrization and 5) required time for calibration (not exceeding 15min).

2.4.1 Surface Laplacian

The Surface Laplacian (SLap) is a spatial filter and BCI paradigm based on the design of the Graz brain-computer interface [22], in which left and right motor images were used to generate specific brain-signals. The model uses non-adaptive and non-data driven spatial filter the Surface Laplacian [24],[35], and a non-adaptive spectral filter set to from 6 to 32Hz. The Surface Laplacian was implemented by using the five-point approximation method introduced by Hjorth in 1975 [24] and can be expressed as follows:

$$M_j^{Lap} = M_j - \frac{1}{4}\sum_{k\in N_j} M_k, \quad (2)$$

where M_j is the scalp potential EEG of the jth channel, and N_j is an index set of the four adjacent channels (i.e. FC3,C5,C1,CP3 and FC4,C6,C2,CP4 are four surrounding channels of the C3 and C4 respectively). The filter also acts as a spatial high pass filter, and because of its properties, it enhances neuronal activity on the channels close to the motor cortex (C3 & C4) [37–39] and at the same time, it reduces the diffused non-task related oscillatory activity [15]. However, it is robust to the non-stationarity of the data and high power EEG artifacts [23]. It also served as the idea for further data-driven and adaptive algorithms, such as Common Spatial Patterns (CSP) and its further derivatives (FBCSP, SpecCSP etc).

2.4.2 Filter Bank Common Spatial Patterns - (FB)CSP

The CSP (Common Spatial Pattern) paradigm [19] is an extension of Slap, and it is initially described in [40] and applied to EEG in [41]. The improvement of this modelling is adaptive data-driven filtering which is computed using the CSP algorithm. The adaptive filtering projects the original channel space onto new lower dimension space. The linear mapping is obtained by optimizing the variance (power) to be maximally informative with respect to the MI task. The algorithm uses the pre-class signal covariance matrices and solves generalized eigenvalue problem. The FBCSP can be seen as an extension of the basic CSP approach. A series of spatial filters are implemented for different frequency subranges Figure 2, thus creating a specific CSP for a narrow band that suits the oscillatory processes in different frequency bands and on distinct spatial locations.

One additional implementation named FBCSPT (FBCSP Time) extends the idea to the time domain (Figure 2), where for each spectral subband is paired with the temporal windows. The FBCSPT, in that case, captures not only complex EEG dynamics in the spatial and frequency domain, but extends to the interaction between bands in frequency, spatial and time domain. In summary, for CSP the following configuration was used: bandpass filter 6-32Hz with 3 patterns per class. In the case of FBCSP, there are 6 subbands in the range of 6-32Hz with 6Hz bandwidth and 2Hz overlap, followed by a 7th covering the whole spectra, therefore, there are 3 patterns per class per filter. In the case of FBCSPT, the same configuration of FBCSP was used accompanied by the time-windows as in Figure 2.

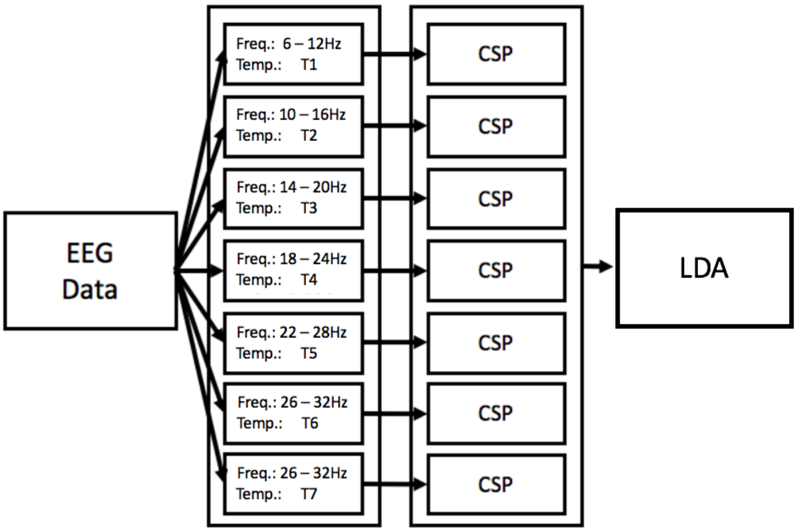

Figure 2. Schematic representation of FBCSP spatial filtering configuration (FBCSP $T1, \ldots, T7 = 0.5 - 4.5\ sec$, FBCSPT $T1, T2 = 0.5 - 3.0 sec, T3, T4, T5, T6 = 1.5 - 4.5 sec, T7 = 0.5 - 4.5 sec$)

2.4.3 Spectrally Weighted Common Spatial Patterns

The Spectrally Weighted Common Spatial Patterns **(**SpecCSP) [19,20] is an advanced paradigm for oscillatory processes using the spectrally weighted CSP algorithm. The approach is designed for the most oscillatory processes and generally gives better results for MI-based BCI than a CSP with a suitably unrestricted spectral filter (e.g. wideband) [19,20]. Therefore, it is useful in cases where the frequency band and conjectured oscillatory activity is unknown. The algorithm optimizes the variance (power) to be maximally informative by the iterative alternation of spectral and spatial filters. The most significant disadvantage of this approach is that it is slower than CSP [20] though in some implementations it is possible to reduce the search space by introducing a prior of the expected location and spectral band, as in the case of MI where the spectral prior is set in the range 6 to 32Hz producing 3 patterns per class.

2.4.4 Spectrally Weighted Regularized Common Spatial Patterns

This approach is a combination of the RCSP [16] and the SpecCSP [19,20] approaches. The Spectrally Weighted Regularized Common Spatial Patterns (SpecRCSP) is an extension of the standard CSP and Tikhonov Regularized CSP (TRCSP) [42] methods to include covariance shrinkage. In addition to the regularization mentioned above instead of the Welch spectral estimate method [47], this approach uses multi-taper spectral estimation [43]. The drawback of SpecRCSP is that it is significantly slower than CSP, but in the case of the Motor Imagery, the search space can be optimized by providing a spectral band that comprises alpha and beta (6 to 32Hz). Similar approaches that can adapt the spectral features to a process of interest are Common Sparse Spectral Spatial Pattern [18], r^2-based heuristics [17], partially based on cross-validation automated parameter search or semi-automated selection based on user's visual feature inspection. The Dual-Augmented Lagrange paradigm is one of the competitive methods specialized in the domains of the complex frequency band interaction and time domain dynamics [44,45], however, the results are not comparable to spatial filtering techniques because the approach merges the classification and optimization strategies, and cannot be used with the same classifier as other methods. For SpecRCSP we set the spectral prior from 6 to 32Hz, with 3 patterns per class, and for power estimation the number of tapers we set to 10. The covariance shrinkage and Tikhonov Regularization applied in SpecRCSP have been tuned by solving the problems analytically

2.4.5 Source Power Comodulation

The Source Power Comodulation (SPoC) approach [46,47] has been designed to decompose EEG data into components using a target variable to guide decomposition. This approach has advantages over blind source separation methods since it has more information to guide separation. SPoC can be seen as further development of the CSP, but instead being applied to the raw EEG data (sensor space), it incorporates source component decomposition. The result of BCI modelling is a set of spatial filters which optimize the co-modulation between the target and the power time course of the spatially filtered EEG signal.

The advantage of the SPoC approach is the presence of the target variable, a scalar function of time, that can be defined as a behavioural measure as the output of the central nervous activity (e.g. sensory response, reaction time, motor and visually evoked potentials, etc.) or parameters of stimulus, where the goal is to correlate stimulus properties with the neuronal properties, or binary as in the case of MI and “rest”.

2.5 Shrinkage Linear Discriminant Analysis Classifier

The log variance features obtained by using each of the aforementioned approaches were fed into the sLDA (Shrinkage Linear-Discriminant Analysis) classifier.

The sLDA was chosen as one of the most popular types of classifiers for EEG based-BCIs [48]. The shrinkage sLDA classifier [49,50] has been shown to be effective with little training data, and thus effective for EEG-based BCI design. The shrinkage parameter was obtained by optimizing the problem analytically.

A dedicated free repository has been created under https://github.com/miladinovic/BCILabTS where the demonstration of implemented BCI pre-processing and spatial filtering techniques is available for further improvement and uses.

2.6 Performance evaluation and Statistical analysis

The classification accuracy on the calibration set was estimated using 10-fold chronological/blockwise cross-validation with 5 trials margin. In 10-fold cross-validation, the calibration dataset containing in total 70 task repetitions was partitioned into ten subsamples. The 9 of 10 subsamples were used to train the model, while the remaining tasks were considered for validation in each run. The process was then repeated 10 times, using each of the subsamples only once as the validation data. Therefore the overall cross-validation accuracy was calculated as a mean of all 10 validation folds (i.e., including the whole 20 min period). Subsequently, the accuracy of created models was calculated on the unseen data test set and compared to those obtained by 10-fold cross-validation on the calibration set.

The aforementioned evaluation procedure was performed firstly without SSA pre-processing, as a standard procedure, and secondly with SSA pre-processing. The difference between the estimated calibration set and real accuracy on tests were assessed by using the Wilcoxon signed-rank test.

3. Results

Median and interquartile range (IQR) values of accuracies observed for each BCI approach, with and without SSA, on calibration and test dataset, as well as their comparison, are reported in Table 1. Figure 3 reports a comparison between the accuracies obtained on the calibration and test data without SSA (Figure 3A), the same comparison obtained with SSA pre-processing (Figure 3B), as well as comparison of performance on test set with and without SSA (Figure 3C).

In Figure 3A it can be observed a large dispersion around the identity line with a trend of lower accuracy on test dataset especially in CSP, SPoC and SpecRCSP. Indeed, classification accuracy resulted significantly lower on test dataset compared to calibration in CSP, SPoC and SpecRCSP (p-value = 0.028, 0.035 and 0.016, respectively). For SLap, SpecCSP only a slight decreasing trend was observed, while FBCSP and FBCSPT maintained moderately high median accuracy >70% (Table 1). In the case of application of SSA pre-processing the differences between accuracy observed on calibration and test dataset were reduced for all methods except SLap approach (Table 1, Figure 3B). In addition, accuracy values both on calibration and test set were slightly higher in case of SSA pre-processing (Figure 3C, Table 1) and also in this case FBCSP and FBCSPT presented slightly better performance compared to other methods.

Table 1. Median and IQR values of accuracies calculated for each BCI approach, with and without SSA pre-processing, on calibration and test dataset, as well as their comparison. IQR- interquartile range; * p-value<0.05.

	SLap	CSP	FBCSP	FBCSPT	SPoC	SpecCSP	SpecRCSP
Accuracy (%) calib - Median (IQR)	69.2 (61.3-76.9)	74.2 (68.1-85.4)	72.5 (62.3-80.6)	74.2 (62.3-82.5)	74.2 (67.5-85.4)	69.2 (61.7-77.7)	71.7 (58.1- 77.5)
Accuracy (%) test - Median (IQR)	64.1 (55.8-72.5)	66.7 (57.7-82.1)	70.2 (58.4-87.8)	74.1 (58.4-80.8)	66.7 (57.7-80.1)	66.7 (53.2-74.4)	59.0 (51.3-71.8)
calib vs test (p-value)	0.381	0.028*	0.636	0.813	0.035*	0.356	0.017*
	+SSA pre-processing						
	SSA+SLap	SSA+CSP	SSA+FBCSP	SSA+FBCSPT	SSA+SPoC	SSA+SpecCSP	SSA+SpecRCSP
Accuracy (%) calib - Median (IQR)	72.0 (61.5-78.9)	75.7 (66.0-82.9)	76.0 (70.0-81.4)	74.3 (69.6-81.1)	75.7 (66.0-82.9)	72.9 (60.0-82.1)	70.0 (54.2-81.1)
Accuracy (%) test - Median (IQR)	64.3 (57.4-72.9)	71.4 (63.6-81.6)	74.3 (70.0-80.7)	75.7 (62.1-82.2)	71.4 (62.7-84.8)	68.6 (63.6-81.6)	67.1 (60.4-76.3)
calib vs test (p-value)	0.085	0.158	0.486	0.408	0.140	0.772	0.938

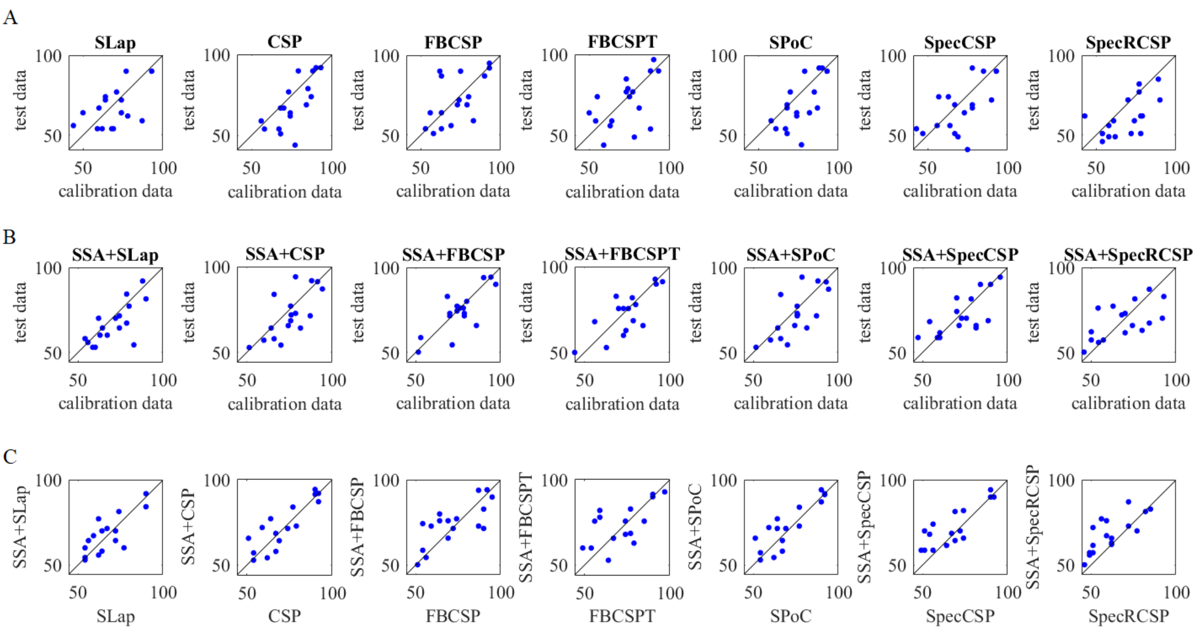

Figure 3. (A) Comparison between accuracy obtained on calibration and test data for each BCI approach. (B) Comparison between accuracy obtained on calibration and test data for each BCI approach after the Stationary-Subspace Analysis (SSA) pre-processing (C) Comparison of accuracy obtained on test data between before and after applying SSA pre-processing for each BCI approach.

4. Discussion

In everyday practice, BCI online sessions are performed at least 20 minutes after the initial calibration session and therefore intrinsic signal nonstationarity characteristic for extracted EEG features may compromise BCI performance. This study evaluated the performance of several spatial-filtering approaches on calibration and test set acquired 30 min after the calibration, mimicking the real BCI scenarios.

The main finding of this study is that EEG extracted feature nonstationarities lead to the BCI model accuracy deterioration, even after 30 minutes of a break. These feature changes had a different impact on the selected spatial filtering approaches. CSP, SPoC and SpecRCSP showed significantly lower accuracy on the test set compared to estimated accuracy on the calibration set. On the other hand, FBCSP and FBSCPT showed to be more robust to feature covariance shift largely maintaining the original performance characterized by moderately high accuracy. Furthermore, we showed that the models produced after SSA pre-processing better maintained the classification performance and, thus, reduced the gap between calibration and test set accuracies. The effect of the SSA pre-processing confirms the existence of nonstationarity caused by covariance shift which violates Machine-Learning basic assumptions of invariant feature distribution between calibration and test test.

The origin of EEG power feature nonstationarities may be caused by various events, such as changes in the participant's attention, fatigue due to the task of electrode placement related [51]**.** Furthermore, the nonstationarity is also related to the change in neural assemblies that are related to the requested cognitive task [52]. In addition, it is well-known that due to non-stationarity based covariate shifts, the input data distributions of EEG-based BCI systems change during inter- and intra-session transitions, which poses great difficulty for developments of online adaptive data-driven systems [34]. Although the aforementioned causes of EEG nonstationarity, that could contribute to performance deterioration over time, are well known, there is little data on how different spatial filtering techniques behave in response to it.

In this study we quantified the performance decline of widely used spatial filtering methods on the dedicated 30min delayed experimental dataset. The assessed decline points out the importance of a more appropriate evaluation framework in order to evaluate the real-life BCI performance. The results also suggest the use of methods which are intrinsically more robust to the EEG nonstationarities, as well as the pre-processing techniques as SSA. The improvement obtained after the application of the SSA confirmed the covariance shift presence and its impact on the observed performance decline.

The overall better performance of FBCSP can be explained by its mechanism that allows capturing interactions between frequency subbands, and in the case of FBCSPT additional interaction of temporal dynamics in defined time-frequency windows. These interactions, at least at the level of the spatial-filter design, are not captured by SLap, SPoC and CSP. Although, that data driven spatial-filtering techniques discard a part of non-stationarity by optimizing the variance only in relation to the experimental task, this process is not guaranteed. We can observe that FBCSP and FBCSPT are less prone to the time-varying effect probably due to intrinsic data-driving mechanisms that operate on small frequency subbands. Despite their moderately higher performance, the FBCSP objective function is defined to optimize variance (power) and not to eliminate feature covariance shifts, as in the case of SSA. Figure 4 demonstrates the effect of SSA pre-processing applied before spatial filtering. We can observe that the covariance of the features are less prominent and that nonstationarities are reduced.

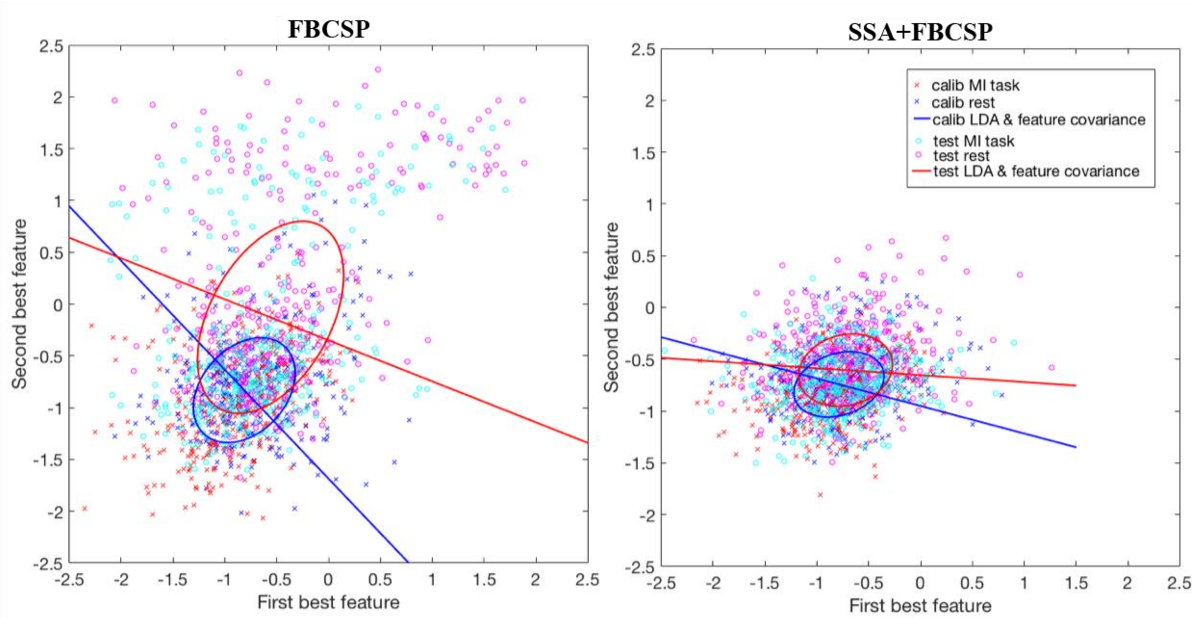

Figure 4. Feature covariance shift of FBCSP (right panel) and with SSA pre-processing (left panel). The blue lines depicts the LDA class separation boundary produced on the calibration set, whilst the red line represents the LDA boundary fit on the test set.

The study shows that there are considerable differences between estimated accuracy using cross-validation and the accuracy obtained on the separate test set. This implies that standardization of the BCI validation framework is required. Establishing a clear validation framework is even more important for evaluation of BCI approaches on clinical populations where due neurophysiological patalogies alternation of oscillatory activity might be present [53]. Furthermore, it is notable that preprocessing with SSA reduces the gap, suggesting that this step should become a part of standard signal processing pipeline for BCI purposes. Additionally, SSA preprocessing can facilitate session-to-session or subject-to-subject transfer learning, by increasing the calibration dataset and reducing the time spent on initial calibration set before the experiment. However, the consideration of only the stationary part of the signal might introduce a decrease of discriminative power of the BCI models. The nonstationarity cannot always be treated as undesirable, since it might also represent positive changes in biological systems, such as, learning neuroplasticity, improvement of motor-imagination skills, increase of attention during experimental time, etc. As a proof-of-concept in our study we fixed the portion of non-stationarity sources, but we believe that carefully selected proportion as a trade-off of BCI discriminatory power and neurophysiological goal (i.e. motor rehabilitation, increase of attention, etc) for each approach and subject will yield to better performance. Therefore, the development and use of BCI models must often balance various competing objectives.

Furthermore, it is worth mentioning that certain types of regularization usually sacrifice train accuracy for generalization, and hypothetically reduces the gap between estimated and real performance of a BCI model. Therefore, the regularization on the level of the classifier, as suggested in recent review, should be always preferred [48]. Additionally, the introduction of some a priori knowledge can increase model performance on unseen test data and create more robust BCI models. Penalizing the channels that are irrelevant for the task proposed in [54], increases overall model accuracy. A selection of the temporal aspect (i.e. the starting points of the time windows of MI task for both training and testing samples) as proposed in [55,56] can further improve model accuracy and possibly make BCI models less affected by the power feature covariance shift.

The limitation of this study is that each participant has performed only one BCI session, preventing us to investigate how SSA pre-processing and spatial filtering techniques behave during the transfer learning. The small number of channels is a limitation since it prevents us from exploring in more detail the neuro plausibility of the generated features. However, the results are obtained on a dedicated dataset acquired to demonstrate the real-life BCI scenario.

5. Conclusions

The results of this study showed that intrinsic signal nonstationarity characteristics, caused by covariance shifts of power features, reduce the accuracy of BCI model on the data acquired 30 minutes after the BCI calibration, suggesting that this evaluation framework should be considered for testing simulating real life performance. FBCSP and FBSCPT approaches showed to be more robust to feature covariance shift largely maintaining the original performance characterized by moderately high accuracy. Stationary Subspace Analysis pre-processing can improve the model performance and reduce accuracy decline from calibration to test set.

Acknowledgments

A. Miladinović is supported by the European Social Fund (ESF) and Autonomous Region of Friuli Venezia Giulia (FVG). Work partially supported by the master programme in Clinical Engineering of the University of Trieste and Interreg V-A Italia-Slovenia 2014-2020 program MEMORI-net.

Conflict of interest

The authors declare that the research was conducted in the absence of any commercial or financial relationships that could be construed as a potential conflict of interest.

References

[1] J. Jarmolowska, M.M. Turconi, P. Busan, J. Mei, P.P. Battaglini, A multimenu system based on the P300 component as a time saving procedure for communication with a brain-computer interface, Front. Neurosci. 7 (2013). https://doi.org/10.3389/fnins.2013.00039.

[2] N. Birbaumer, Breaking the silence: Brain–computer interfaces (BCI) for communication and motor control, Psychophysiology. 43 (2006) 517–532. https://doi.org/10.1111/j.1469-8986.2006.00456.x.

[3] R. Abiri, S. Borhani, E.W. Sellers, Y. Jiang, X. Zhao, A comprehensive review of EEG-based brain–computer interface paradigms, J. Neural Eng. 16 (2019) 011001. https://doi.org/10.1088/1741-2552/aaf12e.

[4] S.M. MASc, A.K.Mas. PhD, A.M.G.M.F. FRCPC, T.C.Mas. PhD, A Review of EEG-Based Brain-Computer Interfaces as Access Pathways for Individuals with Severe Disabilities, Assist. Technol. 25 (2013) 99–110. https://doi.org/10.1080/10400435.2012.723298.

[5] D. Caligiore, M. Mustile, G. Spalletta, G. Baldassarre, Action observation and motor imagery for rehabilitation in Parkinson’s disease: A systematic review and an integrative hypothesis, Neurosci. Biobehav. Rev. 72 (2017) 210–222. https://doi.org/10.1016/j.neubiorev.2016.11.005.

[6] C.L. Friesen, T. Bardouille, H.F. Neyedli, S.G. Boe, Combined Action Observation and Motor Imagery Neurofeedback for Modulation of Brain Activity, Front. Hum. Neurosci. 10 (2017). https://doi.org/10.3389/fnhum.2016.00692.

[7] A. Miladinović, A. Barbaro, E. Valvason, M. Ajčević, A. Accardo, P.P. Battaglini, J. Jarmolowska, Combined and Singular Effects of Action Observation and Motor Imagery Paradigms on Resting-State Sensorimotor Rhythms, in: J. Henriques, N. Neves, P. de Carvalho (Eds.), XV Mediterr. Conf. Med. Biol. Eng. Comput. – MEDICON 2019, Springer International Publishing, Cham, 2020: pp. 1129–1137. https://doi.org/10.1007/978-3-030-31635-8_137.

[8] J.J. Daly, J.R. Wolpaw, Brain–computer interfaces in neurological rehabilitation, Lancet Neurol. 7 (2008) 1032–1043. https://doi.org/10.1016/S1474-4422(08)70223-0.

[9] D.J. McFarland, J. Daly, C. Boulay, M.A. Parvaz, Therapeutic applications of BCI technologies, Brain-Comput. Interfaces. 4 (2017) 37–52. https://doi.org/10.1080/2326263X.2017.1307625.

[10] K.K. Ang, C. Guan, K.S.G. Chua, B.T. Ang, C.W.K. Kuah, C. Wang, K.S. Phua, Z.Y. Chin, H. Zhang, A clinical evaluation of non-invasive motor imagery-based brain-computer interface in stroke, in: 2008 30th Annu. Int. Conf. IEEE Eng. Med. Biol. Soc., IEEE, Vancouver, BC, 2008: pp. 4178–4181. https://doi.org/10.1109/IEMBS.2008.4650130.

[11] J. Mercado, I. Espinosa-Curiel, L. Escobedo, M. Tentori, Developing and evaluating a BCI video game for neurofeedback training: the case of autism, Multimed. Tools Appl. 78 (2019) 13675–13712. https://doi.org/10.1007/s11042-018-6916-2.

[12] A. Miladinović, M. Ajčević, P.P. Battaglini, G. Silveri, G. Ciacchi, G. Morra, J. Jarmolowska, A. Accardo, Slow Cortical Potential BCI Classification Using Sparse Variational Bayesian Logistic Regression with Automatic Relevance Determination, in: J. Henriques, N. Neves, P. de Carvalho (Eds.), XV Mediterr. Conf. Med. Biol. Eng. Comput. – MEDICON 2019, Springer International Publishing, Cham, 2020: pp. 1853–1860. https://doi.org/10.1007/978-3-030-31635-8_225.

[13] D. Brandeis, Neurofeedback training in ADHD: More news on specificity, Clin. Neurophysiol. 122 (2011) 856–857. https://doi.org/10.1016/j.clinph.2010.08.011.

[14] C.S. Nam, A. Nijholt, F. Lotte, Brain–Computer Interfaces Handbook: Technological and Theoretical Advances, CRC Press, 2018.

[15] D.J. McFarland, L.M. McCane, S.V. David, J.R. Wolpaw, Spatial filter selection for EEG-based communication, Electroencephalogr. Clin. Neurophysiol. 103 (1997) 386–394. https://doi.org/10.1016/S0013-4694(97)00022-2.

[16] F. Lotte, Cuntai Guan, Regularizing Common Spatial Patterns to Improve BCI Designs: Unified Theory and New Algorithms, IEEE Trans. Biomed. Eng. 58 (2011) 355–362. https://doi.org/10.1109/TBME.2010.2082539.

[17] B. Blankertz, R. Tomioka, S. Lemm, M. Kawanabe, K. Muller, Optimizing Spatial filters for Robust EEG Single-Trial Analysis, IEEE Signal Process. Mag. 25 (2008) 41–56. https://doi.org/10.1109/MSP.2008.4408441.

[18] G. Dornhege, B. Blankertz, M. Krauledat, F. Losch, G. Curio, K.-R. Muller, Combined Optimization of Spatial and Temporal Filters for Improving Brain-Computer Interfacing, IEEE Trans. Biomed. Eng. 53 (2006) 2274–2281. https://doi.org/10.1109/TBME.2006.883649.

[19] R. Tomioka, G. Dornhege, K. Aihara, K.-R. Müller, An iterative algorithm for spatio-temporal filter optimization, in: Verl. Tech. Univ. Graz, Citeseer, 2006.

[20] R. Tomioka, G. Dornhege, G. Nolte, B. Blankertz, K. Aihara, K.-R. Müller, Spectrally weighted common spatial pattern algorithm for single trial EEG classification, Dept Math Eng Univ Tokyo Tokyo Jpn. Tech Rep. 40 (2006).

[21] L. Qin, L. Ding, B. He, Motor Imagery Classification by Means of Source Analysis for Brain Computer Interface Applications, J. Neural Eng. 2 (2005) 65–72. https://doi.org/10.1088/1741-2560/2/4/001.

[22] G. Pfurtscheller, C. Neuper, Motor imagery and direct brain-computer communication, Proc. IEEE. 89 (2001) 1123–1134. https://doi.org/10.1109/5.939829.

[23] J. Kayser, C.E. Tenke, Issues and considerations for using the scalp surface Laplacian in EEG/ERP research: A tutorial review, Int. J. Psychophysiol. Off. J. Int. Organ. Psychophysiol. 97 (2015) 189–209. https://doi.org/10.1016/j.ijpsycho.2015.04.012.

[24] D.J. McFarland, The Advantages of the Surface Laplacian in Brain-Computer Interface Research, Int. J. Psychophysiol. Off. J. Int. Organ. Psychophysiol. 97 (2015) 271–276. https://doi.org/10.1016/j.ijpsycho.2014.07.009.

[25] B. Reuderink, M. Poel, Robustness of the Common Spatial Patterns algorithm in the BCI-pipeline, (2008). https://research.utwente.nl/en/publications/robustness-of-the-common-spatial-patterns-algorithm-in-the-bci-pi (accessed May 6, 2020).

[26] W. Samek, M. Kawanabe, K.-R. Müller, Divergence-Based Framework for Common Spatial Patterns Algorithms, IEEE Rev. Biomed. Eng. 7 (2014) 50–72. https://doi.org/10.1109/RBME.2013.2290621.

[27] M. Grosse-Wentrup, C. Liefhold, K. Gramann, M. Buss, Beamforming in Noninvasive Brain–Computer Interfaces, IEEE Trans. Biomed. Eng. 56 (2009) 1209–1219. https://doi.org/10.1109/TBME.2008.2009768.

[28] S.-H. Park, D. Lee, S.-G. Lee, Filter Bank Regularized Common Spatial Pattern Ensemble for Small Sample Motor Imagery Classification, IEEE Trans. Neural Syst. Rehabil. Eng. 26 (2018) 498–505. https://doi.org/10.1109/TNSRE.2017.2757519.

[29] N. Padfield, J. Zabalza, H. Zhao, V. Masero, J. Ren, EEG-Based Brain-Computer Interfaces Using Motor-Imagery: Techniques and Challenges, Sensors. 19 (2019). https://doi.org/10.3390/s19061423.

[30] H. Raza, D. Rathee, S.-M. Zhou, H. Cecotti, G. Prasad, Covariate shift estimation based adaptive ensemble learning for handling non-stationarity in motor imagery related EEG-based brain-computer interface, Neurocomputing. 343 (2019) 154–166. https://doi.org/10.1016/j.neucom.2018.04.087.

[31] K.K. Ang, C. Guan, K.S.G. Chua, B.T. Ang, C. Kuah, C. Wang, K.S. Phua, Z.Y. Chin, H. Zhang, Clinical study of neurorehabilitation in stroke using EEG-based motor imagery brain-computer interface with robotic feedback, in: 2010 Annu. Int. Conf. IEEE Eng. Med. Biol., 2010: pp. 5549–5552. https://doi.org/10.1109/IEMBS.2010.5626782.

[32] G. Morone, I. Pisotta, F. Pichiorri, S. Kleih, S. Paolucci, M. Molinari, F. Cincotti, A. Kübler, D. Mattia, Proof of Principle of a Brain-Computer Interface Approach to Support Poststroke Arm Rehabilitation in Hospitalized Patients: Design, Acceptability, and Usability, Arch. Phys. Med. Rehabil. 96 (2015) S71–S78. https://doi.org/10.1016/j.apmr.2014.05.026.

[33] S. Hara, Y. Kawahara, T. Washio, P. von Bünau, Stationary Subspace Analysis as a Generalized Eigenvalue Problem, in: K.W. Wong, B.S.U. Mendis, A. Bouzerdoum (Eds.), Neural Inf. Process. Theory Algorithms, Springer, Berlin, Heidelberg, 2010: pp. 422–429. https://doi.org/10.1007/978-3-642-17537-4_52.

[34] P. von Bünau, F.C. Meinecke, F.C. Király, K.-R. Müller, Finding stationary subspaces in multivariate time series, Phys. Rev. Lett. 103 (2009) 214101. https://doi.org/10.1103/PhysRevLett.103.214101.

[35] P. von Bünau, F.C. Meinecke, S. Scholler, K.-R. Müller, Finding stationary brain sources in EEG data, in: 2010 Annu. Int. Conf. IEEE Eng. Med. Biol., 2010: pp. 2810–2813. https://doi.org/10.1109/IEMBS.2010.5626537.

[36] B. Hjorth, An on-line transformation of EEG scalp potentials into orthogonal source derivations, Electroencephalogr. Clin. Neurophysiol. 39 (1975) 526–530. https://doi.org/10.1016/0013-4694(75)90056-5.

[37] B. He, J. Lian, G. Li, High-resolution EEG: a new realistic geometry spline Laplacian estimation technique, Clin. Neurophysiol. Off. J. Int. Fed. Clin. Neurophysiol. 112 (2001) 845–852. https://doi.org/10.1016/s1388-2457(00)00546-0.

[38] F. Babiloni, C. Babiloni, F. Carducci, L. Fattorini, P. Onorati, A. Urbano, Spline Laplacian estimate of EEG potentials over a realistic magnetic resonance-constructed scalp surface model, Electroencephalogr. Clin. Neurophysiol. 98 (1996) 363–373. https://doi.org/10.1016/0013-4694(96)00284-2.

[39] B. He, Brain electric source imaging: scalp Laplacian mapping and cortical imaging, Crit. Rev. Biomed. Eng. 27 (1999) 149–188.

[40] K. Fukunaga, Introduction to statistical pattern recognition (2nd ed.), Academic Press Professional, Inc., USA, 1990.

[41] H. Ramoser, J. Muller-Gerking, G. Pfurtscheller, Optimal spatial filtering of single trial EEG during imagined hand movement, IEEE Trans. Rehabil. Eng. 8 (2000) 441–446. https://doi.org/10.1109/86.895946.

[42] A. Ashok, A.K. Bharathan, Soujya V.R, P. Nandakumar, Tikhonov regularized spectrally weighted common spatial patterns, in: 2013 Int. Conf. Control Commun. Comput. ICCC, 2013: pp. 315–318. https://doi.org/10.1109/ICCC.2013.6731671.

[43] P.P. Mitra, B. Pesaran, Analysis of dynamic brain imaging data., Biophys. J. 76 (1999) 691–708.

[44] R. Tomioka, M. Sugiyama, Dual-Augmented Lagrangian Method for Efficient Sparse Reconstruction, IEEE Signal Process. Lett. 16 (2009) 1067–1070. https://doi.org/10.1109/LSP.2009.2030111.

[45] A. Miladinović, M. Ajčević, G. Silveri, A. Accardo, Performance of Dual-Augmented Lagrangian Method and Common Spatial Patterns applied in classification of Motor-Imagery BCI, in: Proc. GNB2020, Trieste, 2020: p. 3.

[46] S. Dähne, F.C. Meinecke, S. Haufe, J. Höhne, M. Tangermann, K.-R. Müller, V.V. Nikulin, SPoC: A novel framework for relating the amplitude of neuronal oscillations to behaviorally relevant parameters, NeuroImage. 86 (2014) 111–122. https://doi.org/10.1016/j.neuroimage.2013.07.079.

[47] C. Vidaurre, C. Sannelli, W. Samek, S. Dähne, K.-R. Müller, Machine Learning Methods of the Berlin Brain-Computer Interface, IFAC-Pap. 48 (2015) 447–452. https://doi.org/10.1016/j.ifacol.2015.10.181.

[48] F. Lotte, L. Bougrain, A. Cichocki, M. Clerc, M. Congedo, A. Rakotomamonjy, F. Yger, A review of classification algorithms for EEG-based brain–computer interfaces: a 10 year update, J. Neural Eng. 15 (2018) 031005. https://doi.org/10.1088/1741-2552/aab2f2.

[49] B. Blankertz, S. Lemm, M. Treder, S. Haufe, K.-R. Müller, Single-trial analysis and classification of ERP components — A tutorial, NeuroImage. 56 (2011) 814–825. https://doi.org/10.1016/j.neuroimage.2010.06.048.

[50] F. Lotte, Signal Processing Approaches to Minimize or Suppress Calibration Time in Oscillatory Activity-Based Brain–Computer Interfaces, Proc. IEEE. 103 (2015) 871–890. https://doi.org/10.1109/JPROC.2015.2404941.

[51] Y. Li, H. Kambara, Y. Koike, M. Sugiyama, Application of covariate shift adaptation techniques in brain-computer interfaces, IEEE Trans. Biomed. Eng. 57 (2010) 1318–1324. https://doi.org/10.1109/TBME.2009.2039997.

[52] D. Rathee, H. Cecotti, G. Prasad, Single-trial effective brain connectivity patterns enhance discriminability of mental imagery tasks, J. Neural Eng. 14 (2017) 056005. https://doi.org/10.1088/1741-2552/aa785c.

[53] L. Stragapede, G. Furlanis, M. Ajčević, M. Ridolfi, P. Caruso, M. Naccarato, M. Ukmar, P. Manganotti, Brain oscillatory activity and CT perfusion in hyper-acute ischemic stroke, J. Clin. Neurosci. Off. J. Neurosurg. Soc. Australas. 69 (2019) 184–189. https://doi.org/10.1016/j.jocn.2019.07.068.

[54] J. Jin, Y. Miao, I. Daly, C. Zuo, D. Hu, A. Cichocki, Correlation-based channel selection and regularized feature

optimization for MI-based BCI, Neural Netw. 118 (2019) 262–270. https://doi.org/10.1016/j.neunet.2019.07.008.

[55] J. Jiang, C. Wang, J. Wu, W. Qin, M. Xu, E. Yin, Temporal Combination Pattern Optimization Based on Feature Selection Method for Motor Imagery BCIs, Front. Hum. Neurosci. 14 (2020) 231. https://doi.org/10.3389/fnhum.2020.00231.

[56] J. Feng, E. Yin, J. Jin, R. Saab, I. Daly, X. Wang, D. Hu, A. Cichocki, Towards correlation-based time window selection method for motor imagery BCIs, Neural Netw. 102 (2018) 87–95. https://doi.org/10.1016/j.neunet.2018.02.011.